The Low Frequency All Sky Monitor for the Study of Radio Transients: Array Configuration and Sensitivity

ARCC Scholar thesis

in partial fulfillment of the requirements
of the ARCC Scholar program

Rossina Miller

April 13, 2012

Abstract

The forthcoming Low Frequency All Sky Monitor (LoFASM) will be an array of dipoles working between 10-88 MHz adapted from the Long Wavelength Array (LWA) design. This array will offer significant advantages over other projects for the study of radio transients, but its effectiveness will depend on the geometric details of the array. This thesis presents the results of theoretical sensitivity calculations for a single 12 antenna array. An optimal configuration was found that can effectively block terrestrial signals incident from the horizon at certain "resonant" frequencies. This configuration will allow LoFASM to operate in regions with relatively high radio frequency interference.

Contents

1 Introduction

In the field of radio astronomy, the low frequency band (roughly 10 - 88 MHz) is relatively unexplored. This is due to various historical and technological reasons. Recently, there are several new projects that are investigating this particular frequency range. Such projects include the Long Wavelength Array (LWA) in New Mexico and the Low Frequency Array (Lofar) in Europe. The primary science goals for these instruments include the study of 1) ionospheric, solar and space weather; 2) solar and exosolar planets; 3) cosmic evolution; 4) acceleration, turbulence and propagation of signals in the interstellar medium (ISM) and 5) transient phenomena [1, 2]. The Center for Advanced Radio Astronomy (CARA) in collaboration with the University of New Mexico (UNM) and the Naval Research Laboratory (NRL) are working on an innovative project focusing on radio transients; the Low Frequency All Sky Monitor (LoFASM).

The LoFASM instrument is based on technology developed by the LWA team and will be dedicated to continuous, long-term observations of the low frequency band. The primary science goals of LoFASM will be to study atmospheric, planetary, and astrophysical transient radio events and to design and test radio frequency interference (RFI) mitigation techniques. Of particular interest are transient radio signals emitted by neutron star-neutron star inspirals, neutron star-black hole inspirals, and black hole-black hole inspirals since these inspiral events are also sources of gravitational waves. A coincident detection of such a radio transient together with a gravitational wave event could significantly increase the significance of the gravitational wave detection. In this way LoFASM may play an important role in the first detection of gravitational waves.

LoFASM will consist of four stations, each made up of 12 LWA style antenna stands in a double ring close-packed configuration. The LoFASM stations will be separated by several thousands of kilometers. The first station will be built near Port Mansfield, Texas, 63 miles north of the University of Texas at Brownsville. The second station will be located near the north arm of the VLA in Socorro, New Mexico. The planned location for the third station is near the Cornell University campus in Ithaca, New York. A possible home for the fourth station will be the Owen's Valley Radio Observatory, California. These geographically distinct regions, each observing the same area of sky, will allow LoFASM to quickly determine the origin of a detected signal. A signal detected in all four stations is most likely to be of astro-

nomical origin, while a signal detected at one station and not the others is most likely to be RFI [3]. The antenna stands and front end electronics are identical to those developed by the LWA team. Additional hardware specific to LoFASM, together with the digital processing, are being developed by the Center for Advanced Radio Astronomy's Multipurpose Electronics Lab (CARAMEL) in collaboration with the LWA team.

The proposed placement of the antenna stands within a single LoFASM station can be found in Figure 1 on page 11. The antenna stands will be placed in a close-packed configuration, which consists of two concentric rings of six antenna stands. Following a close-packing of identical spheres, the radius of the outer ring is fixed at $\sqrt{3}$ times the radius of the inner ring. This work shows that this double ring configuration maximizes instantaneous sky coverage at an individual station, while minimizing the effects of RFI originating from the horizon. The double ring configuration allows for some interesting combinations of the signals from the inner and outer rings, which makes the array sensitive to different areas of the sky. When added together in-phase, the region of maximum sensitivity is directly overhead. When added at 180 degrees out of phase (i.e. subtracted from each other) the array will be most sensitive to signals from the horizon. Hence, an analysis of the signals from the two rings will enable one to constrain the zenith angle of a source, thereby allowing one to determine its origin.

The remainder of this thesis is organized in the following way. The different potential sources of radio transients are discussed in Sec. 1.1 which covers the applications of LoFASM. The optimization and validation of the array configuration are then presented in Sec. 2, with the results of these calculations being presented in Sec. 3. Conclusions are given in Sec. 4. Codes showing the functions used to obtain results are relegated to Appendix A.

1.1 LoFASM and Radio Transients

The primary science goal of LoFASM will be to study radio transients. Radio transients are burst of radio radiation that can last from micro-seconds to several days. Some local (within the Solar System) sources of radio transients are energetic particles striking the atmosphere, solar flares, radio bursts from Jupiter's magnetosphere [6] and terrestrial lightning. Other non-local sources of radio transients include magnetic activity on the surfaces of brown dwarfs and particle acceleration in the magnetic fields of flare stars[4, 5]. Radio pulsars are also known to exhibit giant radio pulses de-

tectable in the low frequency band [7], as well as rotating radio transients (RRATs)[12].

Potential, yet currently unconfirmed, sources of radio transients include supernovae, merging neutron stars, coalescing black holes,[8, 9] and Gamma-ray bursts [11]. The most exciting aspect of radio transient work is the unforeseen discovery of unknown sources.

LoFASM may prove to be instrumental in the detection and confirmation of gravitional waves. Neutron star-neutron star inspirals, neutron star-black hole inspirals, and black hole-black hole inspirals are all potential sources of gravitational waves that may also emit a burst of low frequency radio radiation just prior to merger or in the afterglow phase[9]. It has been predicted that the Advanced Laser Interferometer Gravitational-wave Observatory (aLIGO) will see several neutron star-neutron star mergers which LoFASM may be able to confirm by observing the associated radio transient event [10].

LoFASM will also expand the search for radio pulsars, an exotic type of star that emits beams of radio waves from its magnetic poles. Pulsars can exhibit both periodic and transient signals. Unlike normal radio pulsars, RRATs cannot be detected through time-averaged emission and typically last for less than 1 second per day. The spin periods of radio pulsars range from a 1.3 milliseconds to 8.5 seconds [13], while the spin periods associated with RRATs range from 0.4 to 7 seconds[12]. A LoFASM survey should yield around 30 pulsars in the first year, with the possibility of new discoveries. Such a survey would be sensitive to pulsars with periods longer than 0.5 seconds. The new data obtained by LoFASM will help to further our understanding of the basic workings of radio pulsars [14].

2 Theoretical Framework

We are interested in finding the optimal configuration of the LoFASM array in order to maximize its sensitivity to radio transients. In essence, we want the array to see a large portion of the sky and reject signals coming from the horizon, which would most likely be RFI. First we need to calculate the antenna array's "normalized beam pattern" which quantifies the array's sensitivity to a source in a particular direction. Once this is known it will be used to calculate three important statistics that will help determine the

array's effectiveness at detecting transient signals. These statistics will be used to determine the optimal array configuration.

2.1 The Normalized Beam Pattern

The array will be modeled as a set of N antennas, each located at distinct points in space denoted by the displacement vector $\mathbf{x_j}$, where the subscript j runs from 1 to N. Under the plane wave assumption, the electric field at the location of the jth antenna stand is given by

$$\mathbf{E} = E_0 \hat{\mathbf{p}} e^{i(\mathbf{k}\cdot\mathbf{x_j} - \omega t)}, \tag{1}$$

where $\mathbf{k}$ is the wave vector pointing in the direction of propagation, ω is the angular frequency of the wave, E_0 is the scalar amplitude of the wave, and the unit vector $\hat{\mathbf{p}}$ points in the direction of the electric field's polarization. At each antenna, the voltage generated across the terminals by the plane wave is

$$V_j(t) = G_n(\mathbf{k}, \mathbf{p}) E_0 e^{i(\mathbf{k}\cdot\mathbf{x_j} - \omega t)}, \tag{2}$$

where $G_n(\mathbf{k}, \mathbf{p})$ is the antenna's response to the wave, V_{nj} is the and the subscript n denotes the polarization of the antenna. Each antenna stand is made up of two independent dipole antennas, oriented at 90° to each other. The gain of the North-South (East-West) aligned dipoles is given by $G_{NS}(\mathbf{k}, \mathbf{p})$ ($G_{EW}(\mathbf{k}, \mathbf{p})$).

Since we want the maximum sensitivity of the array to be directly overhead, the received signals from all the antenna stands will be added in phase.

The resulting summed signal for a given antenna polarization, S_n, is denoted as

$$S_n = \sum_j V_j(t) = \sum_j G_n(\mathbf{k}, \mathbf{p}) E_0 e^{i(\mathbf{k}\cdot\mathbf{x_j} - \omega t)}. \tag{3}$$

The detected average power in the signal is given by

$$P_n = |S_n|^2 = \sum_{j,l} |G_n(\mathbf{k}, \mathbf{p})|^2 |E_0|^2 e^{i(\mathbf{k}\cdot(\mathbf{x_j} - \mathbf{x_l}))}. \tag{4}$$

The received power for each polarization is given by

$$P_{EW} = \sum_{j,l} |G_{EW}(\mathbf{k}, \mathbf{p})|^2 |E_0|^2 e^{i(\mathbf{k}\cdot(\mathbf{x_j}-\mathbf{x_l}))}, \tag{5}$$

$$P_{NS} = \sum_{j,l} |G_{NS}(\mathbf{k}, \mathbf{p})|^2 |E_0|^2 e^{i(\mathbf{k}\cdot(\mathbf{x_j}-\mathbf{x_l}))}. \tag{6}$$

The total power received will be a sum of the two polarizations.

$$P_T = P_{NS} + P_{EW}. \tag{7}$$

$$P_T = \sum_{j,l} (|G_{NS}(\mathbf{k}, \mathbf{p})|^2 + |G_{EW}(\mathbf{k}, \mathbf{p})|^2) |E_0|^2 e^{i(\mathbf{k}\cdot(\mathbf{x_j}-\mathbf{x_l}))}. \tag{8}$$

We will assume that the source is unpolarized, which means that there is equal power in each of the two possible polarization states. In order to account for this we simply add together the received power in each of the orthogonal polarizations. In this case, the total power takes the form:

$$P_T = \sum_{j,l} A_T(\mathbf{k}) |E_0|^2 e^{i(\mathbf{k}\cdot(\mathbf{x_j}-\mathbf{x_l}))}, \tag{9}$$

where

$$A_T(\mathbf{k}) = |G_{NS}(\mathbf{k}, \mathbf{p_0})|^2 + |G_{EW}(\mathbf{k}, \mathbf{p_0})|^2 + |G_{NS}(\mathbf{k}, \mathbf{p_1})|^2 + |G_{EW}(\mathbf{k}, \mathbf{p_1})|^2. \tag{10}$$

In the above equation, the subscripts on the polarization vectors differentiate between the two polarization states possible for a plan wave traveling in the $\mathbf{k}$ direction. For a crossed-dipole antenna configuration in the long wavelength limit lying in the x-y plane, one can show that

$$A_T = A_0 \left(\frac{1 + \cos(\theta)^2}{2} \right), \tag{11}$$

where A_0 is a constant that depends on the geometry of the antenna and θ is the angle from the z-axis.

Using this one can rewrite Equation 9 as

$$P_T(\theta,\phi) = A_0 \left(\frac{1+\cos(\theta)^2}{2}\right) |E_0|^2 \sum_{j,l} e^{i(\mathbf{k}(\theta,\phi)\cdot(\mathbf{x_j}-\mathbf{x_l}))}, \tag{12}$$

where we have explicitly written the directional dependence in terms of zenith and azimuthal angles, θ and ϕ. Dividing the above equation by its maximum possible value, $A_0|E_0|^2N^2$, we obtain the normalized beam pattern:

$$B(\theta,\phi) = \left(\frac{1+\cos(\theta)^2}{2}\right) \frac{1}{N^2} \sum_{j,l} e^{i(\mathbf{k}(\theta,\phi)\cdot(\mathbf{x_j}-\mathbf{x_l}))}. \tag{13}$$

The normalized beam pattern is the key to understanding the effectiveness of the LoFASM array at detecting radio transients. Matlab codes were developed to calculate this quantity as a function of the array configuration as well as the source location. A knowledge of the normalized beam pattern allows us to calculate the array's minimum detectable flux, the maximum visible volume as well as the horizon rejection, a statistic that determines how well the array rejects signals coming from the horizon.

2.2 Determining the Minimum Detectable Flux

The normalized beam pattern will now be used to determine the minimum detectable flux. Assuming a single source at a sky location given by θ and ϕ, the power per unit frequency received by the array is

$$P_s = A_m B(\theta,\phi) F_s(\theta,\phi), \tag{14}$$

where A_m is the effective area of the telescope, B is the normalized beam pattern and F_s is the source flux per unit frequency.

Radio transients, our main focus, only emit finite bursts of radio waves. These bursts would create an increase in the noise power above that generated by the sky background. The noise power due to the sky background is determined by the following expression:

$$P_n = \int A_m B(\theta, \phi) I_\nu(\theta, \phi) d\Omega, \tag{15}$$

where $I_\nu(\theta, \phi)$ is the specific intensity of the sky. It is typical to model the background radiation coming from the sky as a blackbody with temperature T_{sky}. In this case, it can be shown that [15]

$$I_\nu(\theta, \phi) = \frac{k_b T_{\text{sky}}}{\lambda^2}. \tag{16}$$

where k_b is Boltzmann's constant and λ is the wavelength of the wave at the frequency ν. The equation for the noise power then becomes

$$P_n = A_m \int B \frac{k_b T_{\text{sky}}}{\lambda^2} d\Omega. \tag{17}$$

Since k_b, T_{sys} and λ are not dependent on direction, the power may be written as

$$P_n = \frac{A_m k_b T_{\text{sky}} \Omega_0}{\lambda^2}, \tag{18}$$

where

$$\Omega_0 = \int B d\Omega. \tag{19}$$

Ω_0 is known as the antenna beam solid angle and quantifies the size of the region of the sky that the array can see.

In order for a source to be detectable, the signal power received must be greater than the noise power. Hence, $P_s > P_n$. This leads to the following inequality:

$$A_m B(\theta, \phi) F_s(\theta, \phi) > \frac{A_m k_b T_{\text{sky}} \Omega_0}{\lambda^2}. \tag{20}$$

By solving for $F_s(\theta, \phi)$ one finds that

$$F_s(\theta, \phi) > F_{\min}(\theta, \phi), \tag{21}$$

where $F_{\min}(\theta, \phi)$ is defined as the minimum detectable flux for a source located at θ, ϕ and is given by:

$$F_{\min}(\theta, \phi) = \frac{k_b T_{\text{sky}} \Omega_0}{B(\theta, \phi) \lambda^2}. \tag{22}$$

Since the maximum value of $B(\theta, \phi)$ is 1, the smallest value of the minimum detectable flux is

$$F_{\min} = \frac{k_b T_{\text{sky}} \Omega_0}{\lambda^2}. \tag{23}$$

2.3 Visible Volume

A good measure of how effective an instrument is at detecting transient sources is given by the total volume of space in which a particular source may be detected. This volume may be calculated using the minimum detectable flux and the total luminosity, L, of a source.

Given the measured flux of a source, F, with luminosity, L, the distance between the receiver and the source is given by

$$r = \sqrt{\frac{L}{4\pi F}}. \tag{24}$$

Since $F_{\min}(\theta, \phi)$ is the minimum detectable flux of the receiver, the maximum possible distance that a detectable source could be is given by

$$r_{\max}(\theta, \phi) = \sqrt{\frac{L}{4\pi F_{\min}(\theta, \phi)}}. \tag{25}$$

The total visible volume of space is then given by

$$V = \int \frac{r_{\max}(\theta, \phi)^3}{3} d\Omega. \tag{26}$$

Using Equation 25, the above becomes

$$V = \int \frac{1}{3} \left(\sqrt{\frac{L}{4\pi F_{\min}(\theta, \phi)}} \right)^3 d\Omega = \int \frac{1}{3} \left(\frac{L}{4\pi} \right)^{\frac{3}{2}} F_{\min}(\theta, \phi)^{-\frac{3}{2}} d\Omega. \tag{27}$$

Using Equation 22 for $F_{\min}(\theta, \phi)$, the volume may written as

$$V = \int \frac{1}{3} \left(\frac{L}{4\pi} \right)^{\frac{3}{2}} \left(\frac{B(\theta, \phi)\lambda^2}{k_b T_{\text{sky}} \Omega_0} \right)^{\frac{3}{2}} d\Omega. \tag{28}$$

The only thing dependent on direction is $B(\theta, \phi)$, therefore the volume takes the form

$$V = \frac{1}{3} \left(\frac{L}{4\pi k_b T_{\text{sky}} \Omega_0} \right)^{\frac{3}{2}} \lambda^3 \gamma \tag{29}$$

where γ is defined as

$$\gamma = \int B(\theta, \phi)^{\frac{3}{2}} d\Omega. \tag{30}$$

2.4 Horizon Rejection Factor and Array Optimization

Unwanted signals are most likely to originate from the horizon at high zenith angles. An ideal array would reject such signals while maintaining sensitivity to signals coming from overhead. The integral of the normalized beam pattern over the horizon region, as opposed to over the entire sky, is a measure of the array's sensitivity to signals coming from the horizon. We define the following quantity:

$$H = \int_{\pi/2-\delta<\theta<\pi/2} B(\theta,\phi)d\Omega. \tag{31}$$

where δ is the angle subtended by the horizon, which we will take to be 10°. The ratio of H to the antenna beam solid angle, Ω_0, is a measure of how well the antenna rejects signals from the horizon and admits signals from overhead. We refer to this ratio as the horizon rejection factor. When optimizing the array configuration, one would want to minimize this quantity.

The horizon rejection factor can be directly related to the apparent increase in the sky temperature due to signals from the horizon. Up to now, we have been modeling the sky brightness as an isotropic blackbody with temperature $T_{\rm sky}$. Now we will consider a two component model where the temperature within the horizon region is $T_{\rm sky} + \Delta T_h$ and is $T_{\rm sky}$ elsewhere. For this case, the received noise power becomes

$$P_n = \frac{A_m k_b T_{\rm sky}\Omega_0}{\lambda^2} + \int_{\pi/2-\delta<\theta<\pi/2} \frac{A_m k_b \Delta T_h}{\lambda^2} B(\theta,\phi)d\Omega. \tag{32}$$

Since all the terms under the integral, except for $B(\theta,\phi)$, are independent of θ and ϕ we can rewrite the above equation using Equation 31 as

$$P_n = \frac{A_m k_b T_{\rm sky}\Omega_0}{\lambda^2} + \frac{A_m k_b \Delta T_h H}{\lambda^2}. \tag{33}$$

After factoring, we find that

$$P_n = \frac{A_m k_b T_{\rm sky}\Omega_0}{\lambda^2}\left(1 + \frac{\Delta T_h}{T_{\rm sky}}\frac{H}{\Omega_0}\right), \tag{34}$$

By comparing this result to Equation 18, we see that we can define an equivalent system temperature given by

$$T_{\text{sys}} = T_{\text{sky}}(1 + \frac{\Delta T_h}{T_{\text{sky}}} \frac{H}{\Omega_0}). \tag{35}$$

The noise power induced in the array by this two component non-isotropic sky brightness model is equivalent to the noise power induced by an isotropic sky with temperature T_{sys}.

For the case where the array is located in a low RFI environment, the second term in the parenthesis of Equation 35 is small. Hence, the system temperature is simply the isotropic sky temperature independent of the horizon rejection factor, as expected. In a high RFI environment, the system temperature is dominated by $\Delta T_h H/\Omega_0$. Therefore, minimizing the horizon rejection factor will minimize the total system temperature and hence the receiver noise power.

3 Discussion

This section analyzes the properties of the Double Ring Close-Packed configuration (see Figure 1 on page 11) and shows that it appears to be an optimal configuration to reject unwanted RFI coming from the horizon. The size of the inner radius sets the optimal observing frequency for a station. This configuration allows for two distinct combinations of the signals from the inner and outer rings, which makes the array sensitive to different areas of the sky.

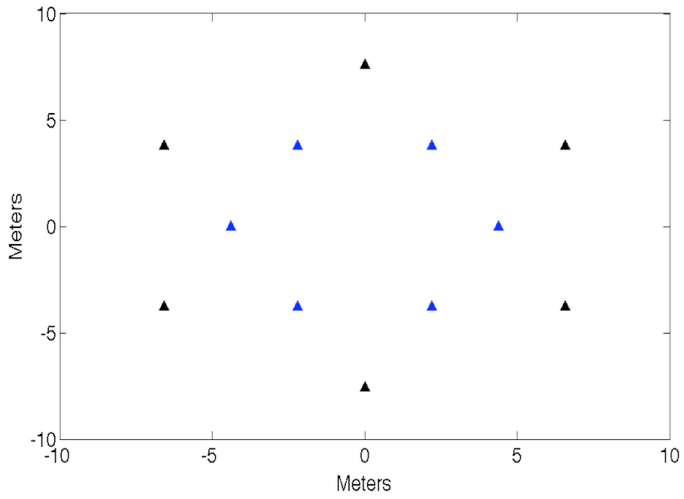

Figure 1: Double Ring Close-Packed Configuration: The radius of the outer ring is fixed at $\sqrt{3}$ times the inner radius. When added together in-phase, the region of maximum sensitivity is directly overhead. When added at 180 degrees out of phase, the array will be most sensitive to signals from the horizon.

3.1 Optimal Arrangement

For a LoFASM station, the system noise is dominated by two sources: the Galactic noise background and local RFI. The ideal design of LoFASM aims, not only to optimize sky coverage, but to be as insensitive as possible to the local RFI. By adding together in phase the received signals from all 12 antennas, one can numerically calculate the normalized power pattern, $B(\theta, \phi)$, for a station. For the particular configuration optimized for 20 MHz, Figure 2 shows the normalized beam pattern at 20 MHz as a function of θ and ϕ, where θ and ϕ are the azimuth and zenith angles, respectively. This is a 3D plot of the surface defined by $B(\theta, \phi)$ as given in Equation 13.

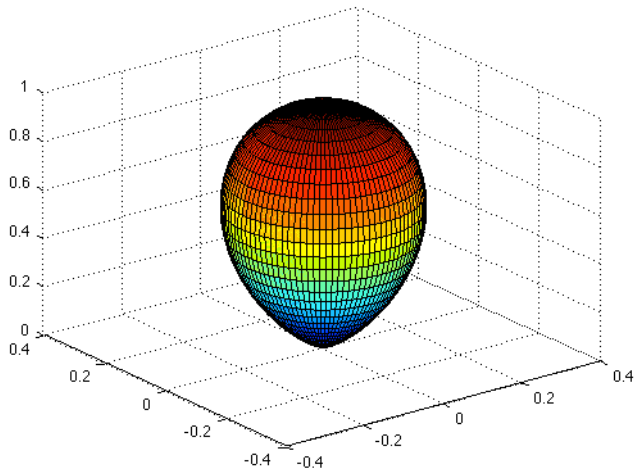

Figure 2: Normalized Beam Pattern at 20 MHz for an array optimized at 20 MHz (i.e. an inner radius of 4.42 m). The color pattern represents the sensitivity, with red being the highest sensitivity and blue being the weakest.

For the purpose of rejecting local RFI, a configuration with the lowest possible H/Ω_0 was selected. In order to determine this for a particular frequency (i.e. 20 MHz), values for the horizon rejection of the double ring configuration were plotted against a range of radii, from 3 to 83 meters, to determine the ideal inner radius (See Figure 3 for page 13).

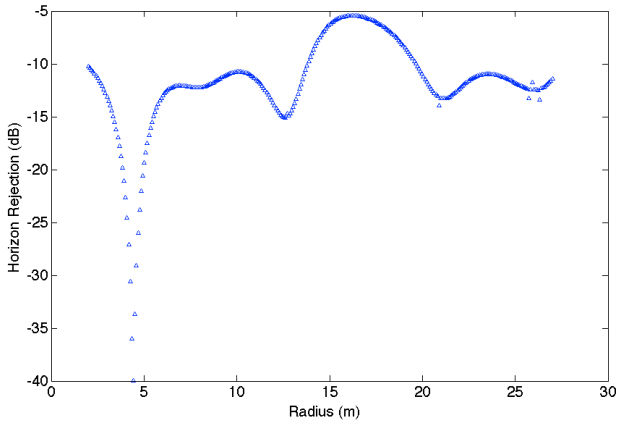

Figure 3: H/Ω_0 was evaluated over a range of radii at a fixed frequency of 20 MHz in order to determine the ideal radius for this frequency. As can be seen in the above figure, the minimum of H/Ω_0 occurs at a radius of 4.42 m.

At 20 MHz, H/Ω_0 is minimized at 4.42 m. The values of the inner radii for frequencies between 5 to 30 MHz can be found in Table 4.1 on page 16.

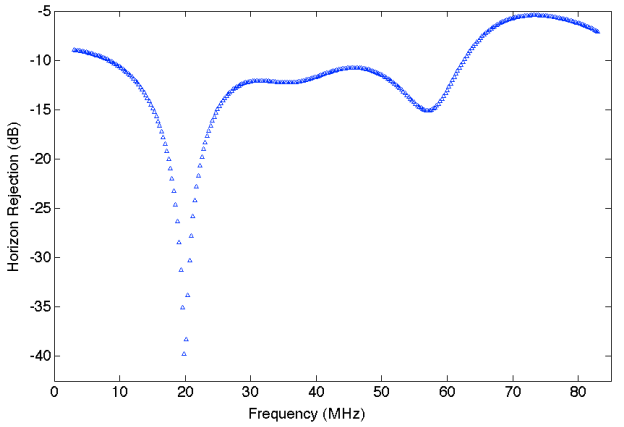

Figure 4: Frequency vs Horizon Rejection: This shows the values of H/Ω_0 for the Double Ring Configuration optimized for 20 MHz. The frequency runs from 3-83 MHz with 300 bins. The magnitude of the highest horizon rejection for 20 MHz, is - 39.5 dB

3.2 Validation of the Double Ring Configuration

To eliminate the possibility that a configuration different than that of the double ring close-packed configuration might have a higher horizon rejection, a Monte-Carlo style analysis was done to test random array configurations. Random configurations of 12 antennas were generated and H/Ω_0 was calculated for each one at a fixed frequency of 20 MHz. Figure 5 below shows the histogram of the H/Ω_0 values for 750,000 trial arrays. The smallest value of H/Ω_0 generated was -8.46 dB, which was much higher than -39.5 dB, the local minimum found with the double ring configuration.

A second test of the double ring configuration was done by looking at small perturbations, no more than a tenth of the wavelength in magnitude, around the existing positions of the antenna stands. This helps determine whether or not the original placement of the double ring configuration is actually optimized for a given frequency. This test was devised because it was determined that it would take roughly 10^{26} different random configurations to get an array that would create a local minimum for H/Ω_0. This method is a more efficient test of the double ring configuration than the Monte-Carlo test.

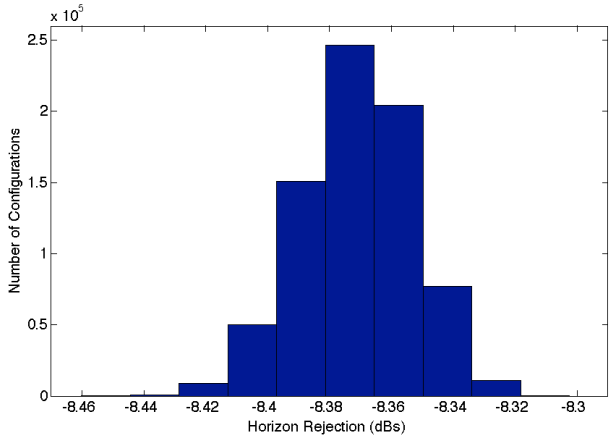

Figure 5: Minimized values of H/Ω_0: This shows the lowest values of H/Ω_0 generated for 750,000 random arrays. The smallest value of H/Ω_0 generated was -8.46 dB.

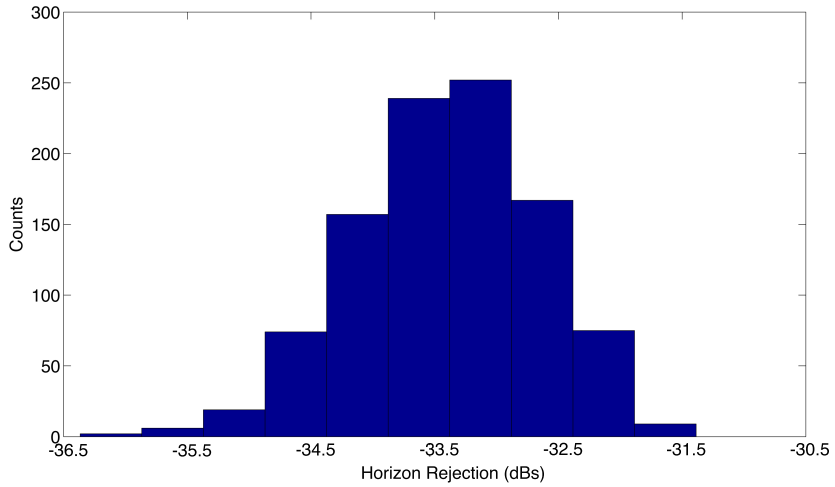

Figure 6: This histogram displays the minimized values of H/Ω_0 generated for the skewed double ring configurations. There were a total of 1000 different iterations and the lowest value was -36.4 dBs.

1000 different perturbations in the double ring configuration were tested (See figure 6 on page 15). The lowest value of H/Ω_0 was found to be -36.4 dBs which is still higher than the local minimum obtained with the double ring configuration. This is strong evidence that the double ring arrangement minimizes H/Ω_0 for a set of 12 antennas, with a higher horizon rejection than other configurations.

4 Conclusion

4.1 What's been accomplished

We calculated the sensitivity and horizon rejection of the array in the double ring configuration optimized for specific frequencies between $5 and 30$ MHz. (See Table 4.1). The radii for each target frequency was also determined. The final tests of the double ring configuration established it as an optimal configuration for observing radio transients. The Monte-Carlo analysis found the smallest value of H/Ω_0 to be -8.46 dB, a much lower level of horizon rejection than the -39.5 dB of the double ring configuration. 1000 different skewed double ring configurations were tested and the lowest value

of H/Ω_0 was found to be -36.4 dBs, a higher value than the local minimum of the original double ring configuration.

Frequency (MHz)	5	10	15	20	25	30
Radius (m)	17.4	8.79	6.04	4.42	3.51	3.01
Volume ($\times 10^{29}$)	1.26	2.21	2.99	3.82	4.17	5.37
H/Ω_0 (dB)	-33.8	-36.8	-36.7	-39.5	-37.2	-37.6
Min Flux ($\times 10^{-20}$ Jy)	5.63	3.77	2.92	2.38	1.98	1.67

4.2 Future Questions

This project did not address the potential issue of mutual coupling. There are two different software packages that could be used in the future to test mutual coupling, NEC3 and Comsol. Both of these can model the properties of the array, as well as each individual antenna stand. It has been suggested that the effects of mutual coupling can be small (private communications with S.W. Ellingson).

In order to truly optimize the double ring configuration longer simulations of both random array tests need to be run. A run of 1 million arrays for each test would give a more accurate picture of the results.

5 Acknowledgments

I am grateful for the guidance provided by my advisor Fredrick Jenet, and all members of the ARCC faculty. I would also like to thank Namir Kassim and Paul Ray (NRL) and Greg Taylor (UNM) for all the feedback and support they gave this project. I thank the Department of Physics & Astronomy at the University of Texas at Brownsville for providing the setting and support that allowed this work to be done. I thank the National Science Foundation for the PAARE grant AST-0545837 that supported the ARCC Scholars program, and hence supported my own education and research.

A Codes

A.1 LoFASM H/Ω_0 Script

Script to plot the horizon rejection over an array of frequencies

```
clear all

%Theta direction of maximum gain
alpha = 0;

%Phi direction of maximum gain
beta = 0;

%Number of antennas in the inner circle
N_i = 6;

%Number of antennas in the outter circle
N_o = 6;

%Generates the array of locations for each antenna,
%each antenna 1 meter away from the other
R = arraydist(N_i,N_o,1,sqrt(3),pi/6);

%phi0 = zeros(1,N_i+N_o);
%
phi0 = 0;

%The direction of maximum gain
K0 = [sin(alpha).*cos(beta) sin(alpha).*sin(beta) cos(alpha)];

%Optimized Radius for 5MHz
%R = 17.4 .* R;
%Optimized Radius for 10MHz
%R = 8.79 .* R;
%Optimized Radius for 15MHz
%R = 6.04 .* R;
%Optimized Radius for 20MHz
R = 4.42 .* R;
%R = 5.763 .* R;
%Optimized Radius for 25MHz
%R = 3.41 .* R;
%Optimized Radius for 30MHz
%R = 3.01 .* R;
```

```
N_freq = 300;

 V = zeros(1,N_freq);
HO = zeros(1,N_freq);
 H = zeros(1,N_freq);
 O = zeros(1,N_freq);
Nu = zeros(1,N_freq);

nu_s = 3;
nu_e = 83;

d_nu = (nu_e - nu_s) / (N_freq - 1);

for i = 0:N_freq-1

    nu = i*d_nu + (nu_s);

    Nu(1,i+1) = nu;

    T_s = 10000 .* (nu/38).^(-2.55);
    T_h = 900 .* T_s;

    [V(1,i+1) H(1,i+1) O(1,i+1)] =
        ArrayVolume2( R, K0, T_h, T_s, nu, phi0 );

    a = i+1
end

%Calculates the minimum value of H/O
minHO = min(10*(log10(H) - log10(O)));

%Plots Frequency vs. Volume
 figure;
 plot(Nu,V,'b^')

 xlabel('Frequency')

 ylabel('Volume')

%Plots Frequency vs. Horizon Rejection
figure;
plot(Nu,HO,'b^')

xlabel('Frequency (MHz)')
```

```
ylabel('Horizon Rejection (dB)')
```

A.1.1 arraydist

```
%This function generates the inner and outer circles of the array
function [R] = arraydist( num_i, num_o, r_i, r_o, offset)

%num_i is the number of antennas in the inner ring
%num_o is the num of antennas in the outer ring
%r_i is the inner radius
%r_o is the outer radius
%offset is the angle of rotation of the outer ring to the inner ring

%The angle between each component
angle_i = 2*pi / num_i;
angle_o = 2*pi / num_o;

%The x,y locations of each component of the inner circle
x_i = zeros(1,num_i);
y_i = zeros(1,num_i);
z_i = zeros(1,num_i);

for j = 1:num_i
    x_i(1,j) = r_i*cos(angle_i + (j-1)*angle_i);
    y_i(1,j) = r_i*sin(angle_i + (j-1)*angle_i);
end

%The x,y locations of each component of the outer circle
x_o = zeros(1,num_o);
y_o = zeros(1,num_o);
z_o = zeros(1,num_o);

for l = 1:num_o
    x_o(1,l) = r_o*cos(angle_o + (l-1)*angle_o + offset);
    y_o(1,l) = r_o*sin(angle_o + (l-1)*angle_o + offset);
end

%The array with all the locations of the antennas
R = [x_i x_o; y_i y_o; z_i z_o;]';

end
```

A.1.2 ArrayHO

```
%This function determines the value of the horizon
%rejection of the array for a given frequency

function [ H, O ] = ArrayHO( R, K0, T_h, T_sky, nu, phi0 )

%R is the antenna distribution
%T_h is the temperature of the horizon
%T_sky is the temperature of the sky
%nu is the frequency

%Boltzmann Constant
K_b = 1.38e-23;

%Wavelength
W = 2.998e2/nu;

%The integral of the gain raised to 3/2
gamma = BeamSize2( R, nu, K0, phi0, 3/2 );

%The integral of the gain over the whole sky
O = BeamSize2( R, nu, K0, phi0, 1 );

%The integral of the gain over the horizon
H = BeamSizeH2( R, nu, K0, phi0, 1 );

end
```

A.1.3 BeamSizeH2

```
%This function that tells us the instantaneous
%field of view of the array
function [ H ] = BeamSizeH2( R, nu, K0, phi0, power )

%array specified by R
%nu corresponds to the frequency
%K0 is the direction of maximum gain
%T is thresold
%phio is
%p is power of the gain
%delta is the angle above the horizon, from pi/2

global bpg_R bpg_K0 bpg_phi0 bpg_nu bpg_power
```

```
bpg_R = R;
bpg_K0 = K0;
bpg_phi0 = phi0;
bpg_nu = nu;
bpg_power = power;

%Integral of the beampattern over the solid angle of the horizon
H = dblquad(@beampatterngenglobal, (4*pi)/9,pi/2, 0,2*pi);

end
```

A.1.4 beampatternglobal

```
%This function generates the normalized beam pattern of the array
function [ output ] = beampatterngenglobal( theta, phi )

global bpg_R bpg_K0 bpg_phi0 bpg_nu bpg_power

R = bpg_R;
K0 = bpg_K0;
phi0 = bpg_phi0;
nu = bpg_nu;
power = bpg_power;

c = 2.998e2;

Ntheta = length(theta);

output = zeros(1,Ntheta);

for j = 1:Ntheta,

K = [sin(theta(j)).*cos(phi(1)) sin(theta(j)).*sin(phi(1)) cos(theta(j))];
K = K.*(2*pi.*nu/c);

%The dot product between K and the
%displacement of each antenna
Kr = K * R';

%The dot product of the direction of maximum gain
%and the displacement of each antenna
K0r = K0 * R';

%Sum of induced voltages
s = sum(exp((1i .* Kr) + (-1i .* K0r) + (1i .* phi0)));
```

```
%number of data points in Kr
N = length(Kr);

%Squared Sum
s2 = (conj(s) .* s)/N^2;

%Unit vector of K
Kh = K/(sqrt(K*K'));

%Gain of the telescope
G_t = 1 + cos(theta(j))^2;

%Power in a certain direction
P = G_t * s2;

output(j) = (P.^power) * sin(theta(j));

end

end
```

A.2 LoFASM H/Ω_0 Script for Random Configurations

```
%script to find values of H/O for Random Configurations

clear all

%Theta direction of maximum gain
alpha = 0;

%Phi direction of maximum gain
beta = 0;

%Number of antennas
num_a = 12;

%Number of antennas in the inner circle
N_i = 6;

%Number of antennas in the outter circle
N_o = 6;

%Generates the array of locations for each antenna,
%each antenna 1 meter away from the other
```

```
R = randarraydist(num_a);
%R = arraydist(N_i,N_o,1,sqrt(3),pi/6);
%RR = randdoublering(num_a);

%phi0 = zeros(1,N_i+N_o);
%
phi0 = 0;

%The direction of maximum gain
K0 = [sin(alpha).*cos(beta) sin(alpha).*sin(beta) cos(alpha)];

%Optimized Radius for 5MHz
%R = 17.4 .* R;
%Optimized Radius for 10MHz
%R = 8.79 .* R;
%Optimized Radius for 15MHz
%R = 6.04 .* R;
%Optimized Radius for 20MHz
R = 4.42 .* R;
%Optimized Radius for 25MHz
%R = 3.41 .* R;
%Optimized Radius for 30MHz
%R = 3.01 .* R;

R = R + RR;

N_freq = 300;

 V = zeros(1,N_freq);
HO = zeros(1,N_freq);
 H = zeros(1,N_freq);
 O = zeros(1,N_freq);
Nu = zeros(1,N_freq);
 min_HO = zeros(1,N_freq);

nu_s = 3;
nu_e = 83;

d_nu = (nu_e - nu_s) / (N_freq - 1);

for i = 0:N_freq-1

    nu = i*d_nu + (nu_s);

    Nu(1,i+1) = nu;
```

```
    T_s = 10000 .* (nu/38).^(-2.55);
    T_h = 900 .* T_s;

    [V(1,i+1) H(1,i+1) O(1,i+1)] =
        ArrayVolume2( R, K0, T_h, T_s, nu, phi0 );

    HO(1,i+1) = H(1,i+1)/O(1,i+1);

    a = i+1
end

figure;
plot(Nu,V,'b^')

xlabel('Frequency (MHz)')

ylabel('Volume')

figure;
plot(Nu,log10(H)-log10(O),'b^')

xlabel('Frequency (MHz)')

ylabel('Horizon Rejection (dB)')
```

A.3 randarraydist

```
function [R] = randarraydist( num_a )

%The x,y,z locations of each antenna stand
x = zeros(1,num_a);
y = zeros(1,num_a);
z = zeros(1,num_a);

for j = 1:num_a
    x(1,j) = 2.*(rand(1,1) - 0.5);
    y(1,j) = 2.*(rand(1,1) - 0.5);
end

%The array with all the locations of the antenna stands
R = [x; y; z]';

plot(x,y,'b^')
```

```
end
```

A.4 minHO

```
%script to plot min H/O for N random arrays
clear all

%Number of antennas
num_a = 12;

%Number of random arrays to try
%N = 750000;
N = 1000;

%Matrix to hold all min H/O
HO_min = zeros(1,N);
 V_max = zeros(1,N);
 limit = -7;

for i = 0:N-1

    [V,HO] = randdoubleringVol(num_a);
    HO_min(i+1) = min(HO);
    V_max(i+1) = max(V);

    if HO_min < limit
    HO_array = [[min(HO) 0 0]; R];
    dlmwrite('HO_array', HO_array, '-append','roffset', 1)
    end
    b = i + 1

end

figure;
hist(HO_min)

figure;
hist(V_max)
```

A.4.1 randdoubleringVol

```
%Calculates the Volume and Horizon Rejection for
%the Skewed Double Ring Configuration
function [V,HO,R] = randdoubleringVol( num_a )
```

```
R = randdoublering(num_a);

N_freq = 160;

phi0 = 0;
K0 = [0 0 1];

 V = zeros(1,N_freq);
HO = zeros(1,N_freq);
 H = zeros(1,N_freq);
 O = zeros(1,N_freq);
Nu = zeros(1,N_freq);

nu_s = 3;
nu_e = 83;

d_nu = (nu_e - nu_s) / (N_freq - 1);

for i = 0:N_freq-1

    nu = i*d_nu + (nu_s);

    Nu(1,i+1) = nu;

    T_s = 10000 .* (nu/38).^(-2.55);
    T_h = 900 .* T_s;

    [V(1,i+1) H(1,i+1) O(1,i+1)] =
        ArrayVolume2( R, K0, T_h, T_s, nu, phi0 );

    HO(1,i+1) = log10(H(1,i+1))- log10(O(1,i+1));

    a = i+1;
end

end
```

A.4.2 randdoublering

```
%Creates a skewed double ring configuration
function [R] = randdoublering( num_a )

%The x,y,z locations of each antenna stand
x = zeros(1,num_a);
```

```
y = zeros(1,num_a);
z = zeros(1,num_a);

for j = 1:num_a
    x(1,j) = rand(1,1)/(15*.1);
    y(1,j) = rand(1,1)/(15*.1);
end

RR = [x; y; z]';

%Generates the double ring configuration
R = arraydist(6,6,1,sqrt(3),pi/6);

%The array with the random perturbation of
%each antenna stand location
R = 4.42*R + RR;

end
```

References

[1] Taylor, G. B. 2007, Highlights of Astronomy, 14, 388

[2] Falcke, H. D., van Haarlem, M. P., de Bruyn, A. G., et al. 2007, Highlights of Astronomy, 14, 386

[3] Bhat, N. D. R., Cordes, J. M., Chatterjee, S., & Lazio, T. J. W. 2005, Radio Science, 40, 5

[4] Berger, E., Ball, S., Becker, K. M., et al. 2001, Bulletin of the American Astronomical Society, 33, 891

[5] Berger, E. 2002, The Astrophysical Journal, 572, 503

[6] Zarka, P. 2004, Plantary and Space Science, 52, 1455

[7] Cordes, J. M., Bhat, N. D. R., Hankins, T. H., McLaughlin, M. A., & Kern, J. 2004, The Astrophysical Journal, 612, 375

[8] Hansen, B. M. S., & Lyutikov, M. 2001, Monthly Notices of the Royal Astronomical Society, 322, 695

[9] Moortgat, J., & Kuijpers, J. 2004, Physical Review D, 70, 023001

[10] Usov, V. V., & Katz, J. I. 2000, Astronomy and Astrophysics, 364, 655

[11] Sagiv, A., & Waxman, E. 2002, The Astrophysical Journal, 574, 861

[12] McLaughlin, M. A., Lyne, A. G., Lorimer, D. R., et al. 2006, Nature, 439, 817

[13] Lorimer, D. R., Kramer, M., Ellis, R., et al. 2005, Handbook of pulsar astronomy, by D.R. Lorimer and M. Kramer. Cambridge observing handbooks for research astronomers, Vol. 4. Cambridge, UK: Cambridge University Press, 2004,

[14] Stappers, B. W., van Leeuwen, A. G. J., Kramer, M., Stinebring, D., & Hessels, J. 2007, WE-Heraeus Seminar on Neutron Stars and Pulsars 40 years after the Discovery, 100

[15] Wilson, T. L., Rohlfs, K.,& Hüttemeister, S. 2009, Tools of Radio Astronomy, by Thomas L. Wilson; Kristen Rohlfs and Susanne Hüttemeister. ISBN 978-3-540-85121-9. Published by Springer-Verlag, Berlin, Germany, 2009.,